Supplementary Material (ESI) for Chemical Communications

Electronic supplementary information

Reversible modulation of π-association between 3,6-disubstituted carbazole ligands in a multistep assembling process

Norie Inukai, Junpei Yuasa*, and Tsuyoshi Kawai*

Graduate School of Materials Science, Nara Institute of Science and Technology, 8916-5 Takayamacho, Ikoma, Nara 630-0192, Japan,

* To whom correspondence should be addressed.

E-mail: tkawai@ms.naist.jp

Experimental Section

General. ^{1}H NMR spectra were measured with JEOL AL-300N FT NMR SYSTEM (300 MHz). Thin layer chromatography (TLC) was performed on aluminum plates coated with aluminum oxide gel 60 F254 (Merck). Chemicals were purchased from Wako Pure Chemical Industries Ltd. and used as received without further purification. Acetonitrile (MeCN) used as a solvent was obtained from Nacalai Tesque. X-ray diffraction profile was collected and analyzed with an X-ray diffractometer (Rigaku R-AXIS RAPID/s) with the Mo Kα radiation.

Spectral Measurements. Formation of Zn^{2+} complexes of $[(Im_2Cz)_4–Zn^{2+}]_2$, $(Im_2Cz)_3–Zn^{2+}$, and $(ImBrCz)_3–Zn^{2+}$ was examined from the UV-vis spectral change of Im_2Cz in the presence of various concentrations of Zn^{2+} by using a Jasco V-660 spectrophotometer. Formation of the $[(Im_2Cz)_4–Zn^{2+}]_2$ and $(Im_2Cz)_3–Zn^{2+}$ complexes was also examined from the fluorescence spectral change of Im_2Cz in the presence of various concentrations of Zn^{2+} by a HITACHI F-4500 Fluorescence spectrometer. The $(Im_2Cz)_3–Zn^{2+}$ and $[(ImBrCz)_3\text{-}Zn^{2+}]$ complexes were detected by ESI-MS. HRMS (ESI-MS) of $[(ImBrCz)_3\text{-}Zn^{2+}]$: m/z calcd. for $\{[Zn(C_{20}H_{16}BrN_3)_3](OSO_2CF_3)\}^+$ ($[M]^+$), 1344.03945; found 1344.03944 (S3). Mass spectra (ESI-MS and FAB-MS) were measured with mass spectrometers (JEOL JMS-700 MStation). All measurements were performed at room temperature. The reactivity of $[(Im_2Cz)_4–Zn^{2+}]_2$ and $(Im_2Cz)_3–Zn^{2+}$ complexes to toluene were investigated respectively by the UV-vis spectral changes of MeCN solutions of Im_2Cz (3.4×10^{-4} mol dm^{-3}) containing Zn^{2+} (1.0×10^{-4} mol dm^{-3}) (Fig. S9a) and that of Im_2Cz (2.5×10^{-4} mol dm^{-3}) containing Zn^{2+} (1.5×10^{-4} mol dm^{-3}) (Fig. S9b) observed upon addition of toluene in the presence of H_2O (0.22 mol dm^{-3}) at 298 K. In the case of $[(Im_2Cz)_4–Zn^{2+}]_2$, the absorption spectrum of $[(Im_2Cz)_4–Zn^{2+}]_2$ was changed to that of free Im_2Cz (Fig. S9a blue line) by the presence of toluene (5.2×10^{-2} mol dm^{-3}), whereas no notable absorption spectrum change was observed in the spectral titration of $(Im_2Cz)_3–Zn^{2+}$ by toluene (0-9.6×10^{-2} mol dm^{-3}) [Fig. S9b]. A small amount of H_2O was added to a MeCN solution of the $Im_2Cz\text{-}Zn^{2+}$ system to stabilize the Zn^{2+} ions dispersed from $[(Im_2Cz)_4–Zn^{2+}]_2$ complex, inducing the equilibrium shift toward the dissociation of $[(Im_2Cz)_4–Zn^{2+}]_2$.

Preparation of 9-ethyl-3,6-bis[(trimethylsilyl)ethynyl]-9-carbazole (1a): To a flask containing $Pd(PPh_3)_2Cl_2$ (180 mg, 0.25 mmol), CuI (30 mg, 0.15 mmol), and 3,6-dibromo-9-ethylcarbazole (3.1 g, 8.6 mmol) were added (trimethylsilyl)acetylene (2.7 g, 18.7 mmol) in diisopropylamine (30 mL) and tetrahydrofuran (50 mL). The flask was then evacuated and backfilled with nitrogen three times. The mixture was stirred at 60 °C under N_2 atmosphere for 14 h and then filtered. The filtrate was extracted with chloroform, washed with brine and dried over $MgSO_4$ and then filtered. The filtrate was concentrated and subjected to column chromatography on silica gel (hexane/chloroform 1:15) to afford a yellow solid (900 mg, 27 %). ^{1}H NMR ($CDCl_3$, 300 MHz): δ 8.20 (s, 2H), 7.58 (d, J = 8.4 Hz, 2H), 7.31 (d, J = 8.4 Hz, 2H), 4.33 (q, J = 7.2 Hz, 2H), 1.42 (t, J = 7.2 Hz, 3H), 0.29 (s, 18H).

Preparation of 9-ethyl-3,6-bis[(1-methyl-1H-imidazol-2-yl)ethynyl]-9-carbazole (Im_2Cz): A 100

ml four necked flask was charged with 2-iodo-1-methylimidazole (770 mg, 3.7 mmol), 9-ethyl-3,6-bis[(trimethylsilyl)ethynyl]-9-carbazole (700 mg, 1.8 mmol), CuI (6.3 mg, 0.03 mmol), PPh_3 (230 mg, 0.88 mmol), and tetra-*n*-butylammonium fluoride (in THF 1 mol/L, 2.8 mL) in THF/ diisopropylamine (20 ml/10 ml). After the solution was degassed by bubbling with N_2 gas for 30 min, $Pd(PPh_3)_2Cl_2$ (57 mg, 0.081 mmol) was added to the reaction flask. Then, the reaction mixture was stirred at 70 °C under Ar atmosphere for 40 hours. The reaction was left to cool and organic phase was extracted with chloroform washed with brine and dried over $MgSO_4$. The filtrate was concentrated subjected to column chromatography on aluminum oxide (chloroform/acetic ether 15:1). Then Im_2Cz was purified by GPC with chloroform and preparative HPLC with acetonitrile. The crude product was recrystallized in acetonitrile to provide yellow solid (570 mg, 44 %). ^{1}H NMR (300 MHz, CD_3CN): δ 8.31 (s, 2H), 7.64 (d, J = 8.4 Hz, 2H), 7.49 (d, J = 8.4 Hz, 2H), 7.06 (s, 2H), 7.00 (s, 2H), 4.35 (q, J = 7.1 Hz, 2H), 3.76 (s, 6H), 1.33 (t, J = 7.1 Hz, 3H). Anal. Calcd for $C_{26}H_{21}N_5$: C, 77.40; H, 5.25; N, 17.36. Found: C, 77.31; H, 4.98; N, 17.51.

Preparation of 3-bromo-9-ethyl-6-((trimethylsilyl)ethynyl)-9H-carbazole (2a): To a flask containing $Pd(PPh_3)_2Cl_2$ (220 mg, 0.31 mmol), CuI (52 mg, 0.27 mmol), and 3,6-dibromo-9-ethylcarbazole (5.6 g, 16 mmol) were added (trimethylsilyl)acetylene (1.8 g, 17.9 mmol) in diisopropylamine (60 mL) and tetrahydrofuran (150 mL). The flask was then evacuated and backfilled with nitrogen three times. The mixture was stirred at 70 °C under N_2 atmosphere for 14 h and was concentrated and subjected to column chromatography on silica gel (hexane/dichloromethane 1:1) to afford a yellow solid (2.2 g, 37 %). ^{1}H NMR ($CDCl_3$, 300 MHz): δ 8.17 (d, J = 1.5 Hz , 1H), 8.15 (d, J = 1.8 Hz, 1H), 7.58 (dd, J = 8.4, 1.5 Hz 1H), 7.54 (dd, J = 8.4, 1.8 Hz, 1H), 7.28 (d, J = 3.3 Hz , 1H), 7.25 (d, J = 3.3 Hz, 1H), 4.31 (q, J = 7.2 Hz, 2H), 1.40 (t, J = 7.2 Hz, 3H), 0.29 (s, 9H).

Preparation of 3-bromo-9-ethyl-6-((1-methyl-1H-imidazol-2-yl)ethynyl)-9H-carbazole (ImBrCz): A 200 ml four necked flask was charged with 2-iodo-1-methylimidazole (560 mg, 2.7 mmol), 9-ethyl-3,6-bis[(trimethylsilyl)ethynyl]-9-carbazole (1.0 g, 2.7 mmol), CuI (88 mg, 0.46 mmol), PPh_3 (350 mg, 1.33 mmol), and tetra-*n*-butylammonium fluoride (in THF 1 mol/L, 4.3 mL) in THF/ diisopropylamine (120 ml/40 ml). After the solution was degassed by bubbling with N_2 gas for 30 min, $Pd(PPh_3)_2Cl_2$ (110 mg, 0.16 mmol) was added to the reaction flask. Then, the reaction mixture was stirred at 70 °C under Ar atmosphere for 20 hours. The filtrate was concentrated and subjected to column chromatography on aluminum oxide (chloroform/hexane 1:1). Then ImBrCz was purified by preparative HPLC with acetonitrile. The crude product was recrystallized in chloroform to provide yellow solid (655 mg, 64 %). ^{1}H NMR (300 MHz, CD_3CN): δ 8.25 (d, J = 1.5 Hz, 1H), 8.19 (d, J = 1.8 Hz, 1H), 7.68 (dd, J = 8.7, 1.5 Hz, 1H), 7.58 (dd, J = 8.7, 1.8 Hz, 1H), 7.38 (d, J = 8.7 Hz, 1H), 7.30 (d, J = 8.7 Hz, 1H), 7.10 (s, 1H), 6.95 (s, 1H), 4.35 (q, J = 7.2 Hz, 2H), 3.84 (s, 3H), 1.43 (t, J = 7.2 Hz, 3H). HRMS (FAB): m/z calcd. for $C_{20}H_{16}BrN_3$ ($[M]^+$), 377.0528; found 377.0528.

^{1}H NMR assignment of $[(Im_2Cz)_4–Zn^{2+}]_2$: Both $[(Im_2Cz)_4–Zn^{2+}]_2$ and $(Im_2Cz)_3–Zn^{2+}$ complexes were

formed in a CD_3CN solution of Im_2Cz (6.8×10^{-2} mol dm^{-3}) containing Zn^{2+} (2.1×10^{-2} mol dm^{-3}) at 298 K. Under these conditions, exchange between $(Im_2Cz)_3$–Zn^{2+} and $[(Im_2Cz)_4$–$Zn^{2+}]_2$ is rapid on the NOE time scale. This makes it difficult to discuss the intramolecular π-stacking interactions of $[(Im_2Cz)_4$–$Zn^{2+}]_2$ in light of an intermolecular through-space magnetic interaction from NOE experiments, but enables us to identify the ^{1}H NMR assignment of $[(Im_2Cz)_4$–$Zn^{2+}]_2$ by ^{1}H NMR, ^{1}H, ^{1}H COSY NMR, and NOE experiments as follow. When irradiated at the doublet peak of 5.73 ppm due to the C_1-H protons of $[(Im_2Cz)_4$–$Zn^{2+}]_2$, NOE signals were detected for the C_1-H protons of $[(Im_2Cz)_4$–$Zn^{2+}]_2$ at 7.52, 7.64, and 7.14 ppm overlapping with the C_1-H proton of $(Im_2Cz)_3$–Zn^{2+} at 7.15 ppm under these conditions. Then, we identified the neighboring C_2-H protons of $[(Im_2Cz)_4$–$Zn^{2+}]_2$ from the ^{1}H, ^{1}H COSY NMR spectrum obtained under the same experimental conditions. In the ^{1}H, ^{1}H COSY NMR spectrum, the doublet peaks at 6.81, 6.97, 7.13, and 7.67 ppm correspond to the C_2-H protons lying next to the C_1-H protons of $[(Im_2Cz)_4$–$Zn^{2+}]_2$ at 7.64, 5.73, 7.52, and 7.14 ppm, respectively. As expected, NOE signals were detected for the C_2-H protons of $[(Im_2Cz)_4$–$Zn^{2+}]_2$ at 6.97, 7.13, and 7.67 ppm, when irradiated at the doublet peak of 6.81 ppm due to the C_2-H proton of $[(Im_2Cz)_4$–$Zn^{2+}]_2$. NOE signals were also detected for the C_4-H protons of $[(Im_2Cz)_4$–$Zn^{2+}]_2$ at 6.55, 8.02 (8H), and 8.19 ppm, when irradiated at the singlet peak of 8.70 ppm due to the C_4-H proton of $(Im_2Cz)_3$–Zn^{2+}. Similarly, NOE signals were observed for the imidazole protons of $[(Im_2Cz)_4$–$Zn^{2+}]_2$ at 6.49, 7.14, 7.19, 7.32, 7.34, 7.38, 7.46, and 7.55 ppm when irradiated at the singlet peak of 7.34 ppm due to the imidazole protons of $(Im_2Cz)_3$–Zn^{2+}. In the presence of high concentrations of Im_2Cz (6.8×10^{-2} mol dm^{-3}) containing Zn^{2+} (2.1×10^{-2} mol dm^{-3}), Im_2Cz forms other minor complexes, which may be higher-ordered complexes with Zn^{2+}. The NOE signals of these complexes are denoted as asterisks in Fig. S5. Although such other minor complexes could not be identified accurately, it should be noted that only $[(Im_2Cz)_4$–$Zn^{2+}]_2$ and $(Im_2Cz)_3$–Zn^{2+} complexes were formed under the experimental conditions as employed for the UV-vis and ^{1}H NMR titration (Fig. 1 and 2a, respectively).

In the preliminary experiment, we tried to determine the crystal structures of these complexes. Despite our systematic screening for suitable crystallization conditions, evaporation rate, solvent, temperature etc (it was a one year trial), unfortunately, we were unsuccessful in our attempts to grow single crystals of these complexes at present. The $[(Im_2Cz)_4$–$Zn^{2+}]_2$ and $(Im_2Cz)_3$–Zn^{2+} complexes can interconvert between them, because these complexes are on a relatively flat potential energy surface (ΔG = 16 kJ mol^{-1} at 298 K). These effects seem to make us difficult to obtain X-ray crystal structures. At the same time, however, this unique assembling feature of Im_2Cz allows us to create new supramolecular systems, where it undergoes reversible conformational changes caused by subtle changes in the environment.

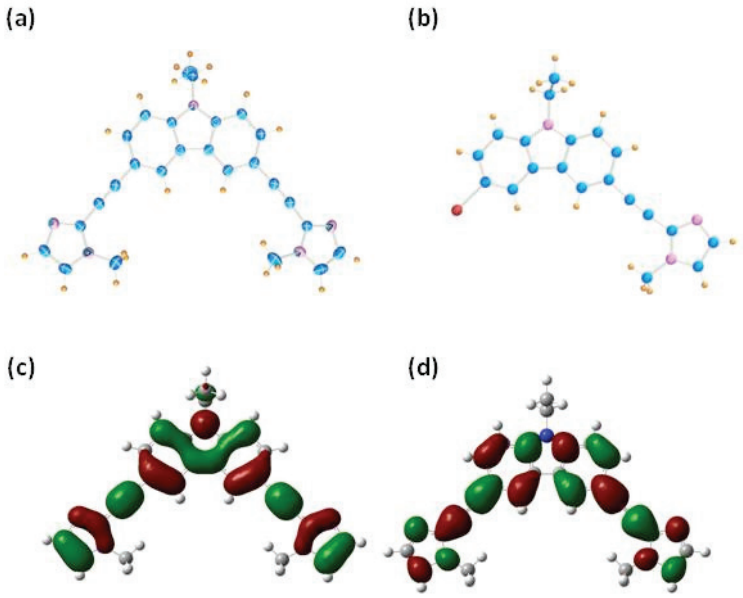

Fig. S1 ORTEP drawing (50% probability) of (a) Im_2Cz and (b) ImBrCz. Color code: blue sphere, C; purple sphere, N; yellow sphere, H; red sphere, Br. (c) HOMO and (d) LUMO orbitals of Im_2Cz calculated by DFT method with Gaussian 03 (B3LYP/6-31G* basis set).

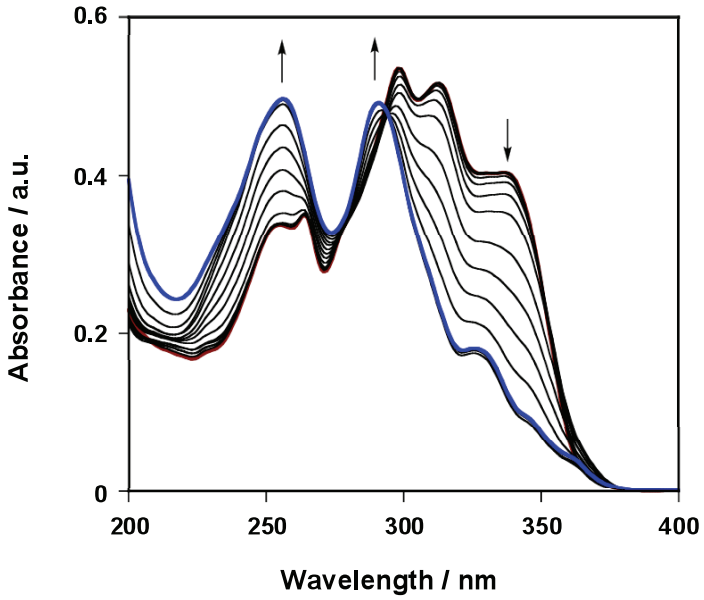

Fig. S2 Observed UV-vis absorption spectral changes upon addition of Zn^{2+} [0 mol dm^{-3} (red line) – 1.3 × 10^{-5} mol dm^{-3} (blue line)] to a MeCN solution of Im_2Cz (2.1 × 10^{-5} mol dm^{-3}) at 298 K.

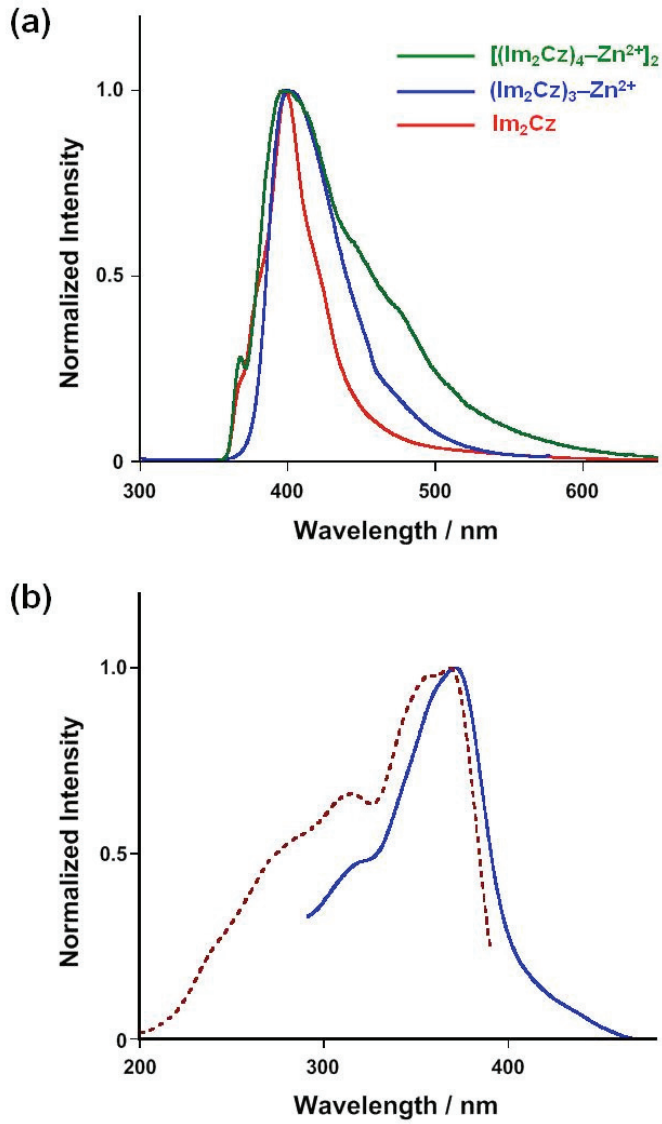

Fig. S3 (a) Normalized emission spectra of Im_2Cz (5.4×10^{-3} mol dm^{-3}) in the absence (red line) and presence of Zn^{2+} (8.1×10^{-4} mol dm^{-3}, green line; 1.6×10^{-3} mol dm^{-3}, blue line) in MeCN at 298 K. (b) Excitation spectra of Im_2Cz (5.4×10^{-3} mol dm^{-3}) in the presence of Zn^{2+} (8.1×10^{-4} mol dm^{-3}) recorded at λ = 550 nm (blue solid line) and 400 nm (red dashed line). *$[(Im_2Cz)_4–Zn^{2+}]_2$ shows a broad emission band due to π-stacked carbazole units at a longer wavelength region overlapping with a emission band due to free carbazole rings.

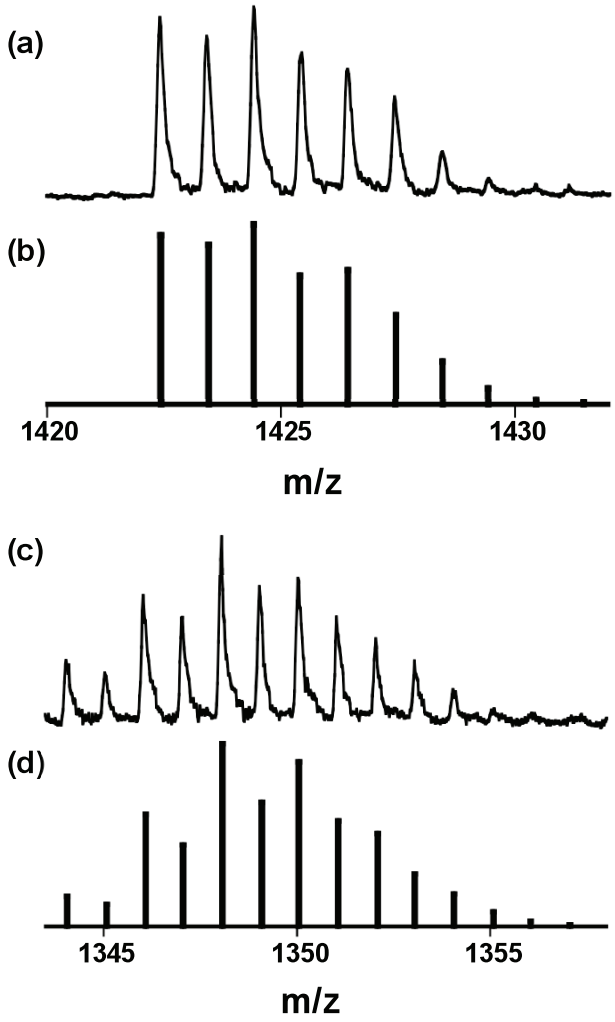

Fig. S4 (a) Positive-ion ESI MS of a MeCN solution of Im_2Cz (2.5×10^{-3} mol dm^{-3}) in the presence of 1.2×10^{-3} mol dm^{-3} of Zn^{2+}. The signal at *m*/*z* 1422.4 corresponds to $\{[Zn(Im_2Cz)_3](OSO_2CF_3)\}^+$. (c) HRMS (ESI-MS) of a MeCN solution of ImBrCz (3.1×10^{-4} mol dm^{-3}) in the presence of 2.1×10^{-4} mol dm^{-3} of Zn^{2+}. The signal at *m*/*z* 1344.0394 corresponds to $\{[Zn(ImBrCz)_3](OSO_2CF_3)\}^+$. (b), (d) Calculated isotopic distributions for $\{[Zn(Im_2Cz)_3](OSO_2CF_3)\}^+$ and $\{[Zn(ImBrCz)_3](OSO_2CF_3)\}^+$, respectively.

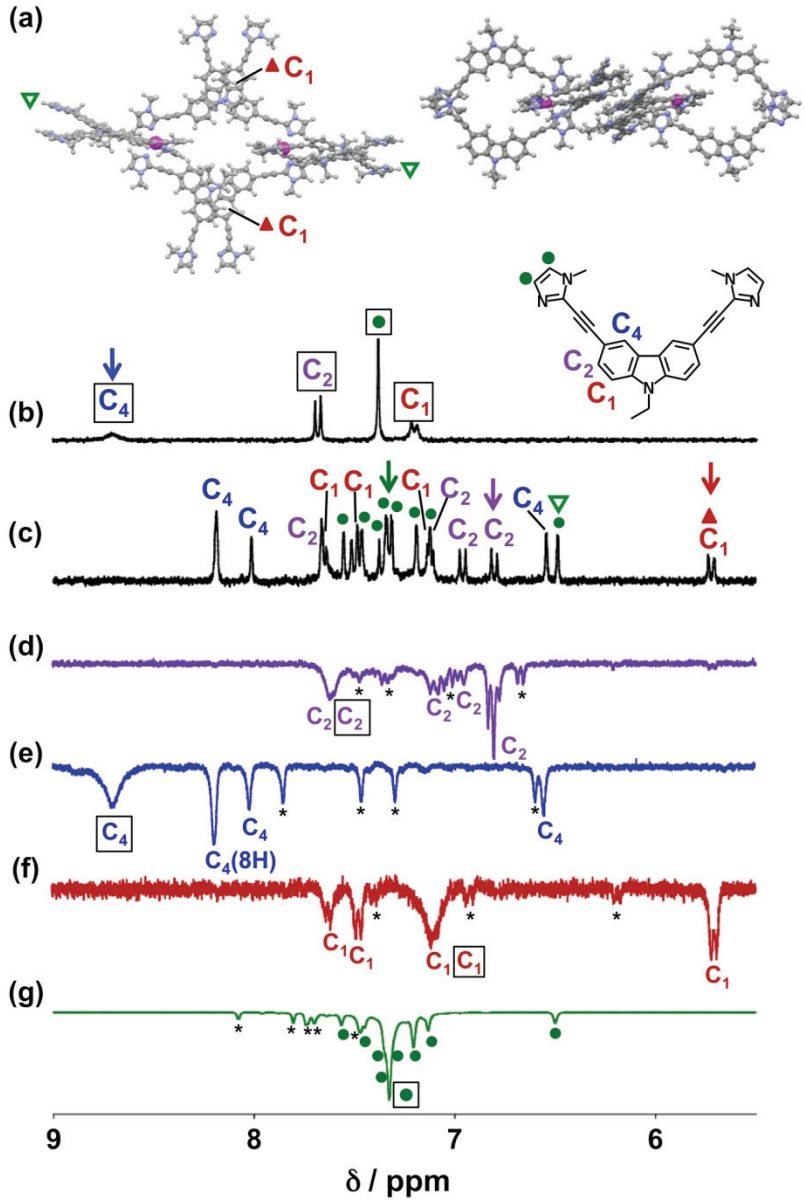

Fig. S5 (a) The structures of $[(Im_2Cz)_4–Zn^{2+}]_2$ modeled by MMFF94: top view (left) and front view (right). ^{1}H NMR spectra of (b) $(Im_2Cz)_3–Zn^{2+}$ and (c) $[(Im_2Cz)_4–Zn^{2+}]_2$ in CD_3CN at 298 K. NOE spectra of a CD_3CN solution of Im_2Cz (6.8×10^{-2} mol dm^{-3}) in the presence of Zn^{2+} (2.1×10^{-2} mol dm^{-3}) at irradiation of (d) the C_2-H of $[(Im_2Cz)_4–Zn^{2+}]_2$ at $\delta = 6.81$ ppm, (e) the C_4-H of $(Im_2Cz)_3–Zn^{2+}$ at $\delta = 8.70$ ppm (f) the C_1-H of $[(Im_2Cz)_4–Zn^{2+}]_2$ at $\delta = 5.73$ ppm, and (g) the imidazole proton of $(Im_2Cz)_3–Zn^{2+}$ at $\delta = 7.34$ ppm in CD_3CN at 298 K. Numbers and symbols correspond to those in the chemical structure of Im_2Cz and the proposed structure of $[(Im_2Cz)_4–Zn^{2+}]_2$. The asterisks denote the NOE signals of other minor complexes.

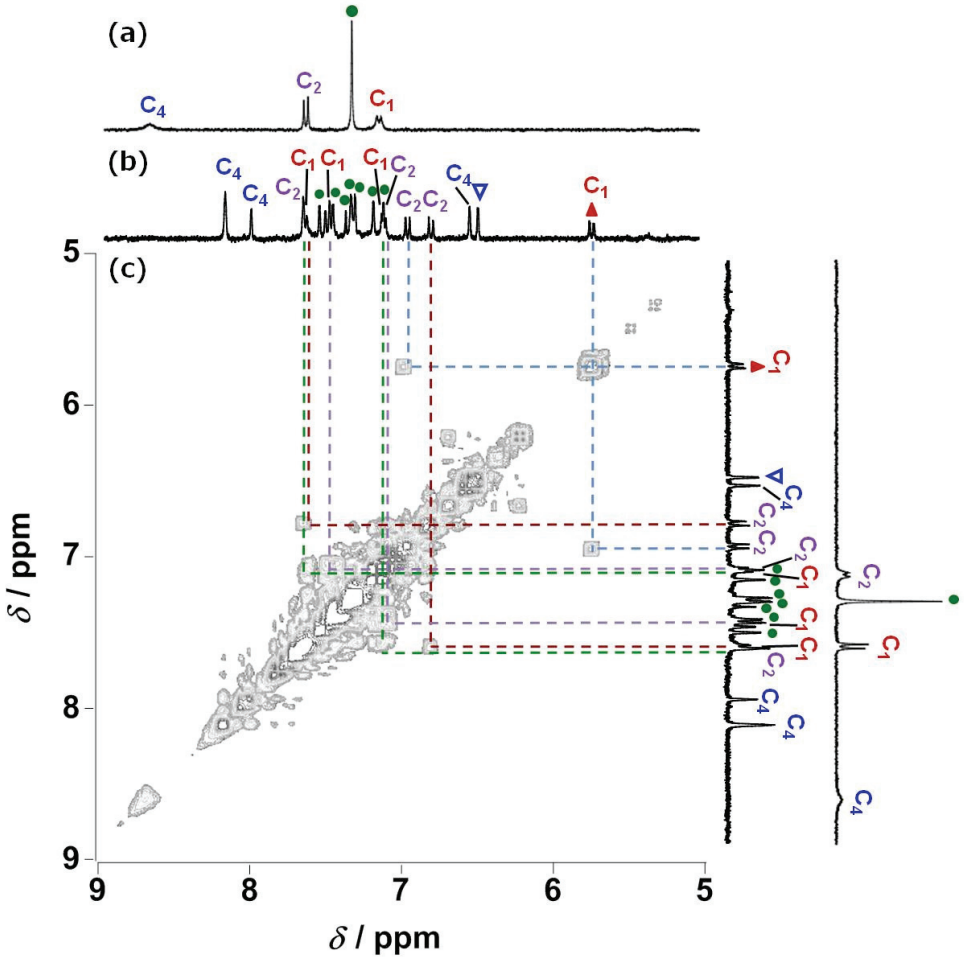

Fig. S6 ^{1}H NMR spectra of (a) $(Im_2Cz)_3$–Zn^{2+} and (b) $[(Im_2Cz)_4$–$Zn^{2+}]_2$ in CD_3CN at 298 K. (c) ^{1}H, ^{1}H COSY NMR spectrum of Im_2Cz (6.8×10^{-2} mol dm^{-3}) in the presence of Zn^{2+} (2.1×10^{-2} mol dm^{-3}) in CD_3CN at 298 K.

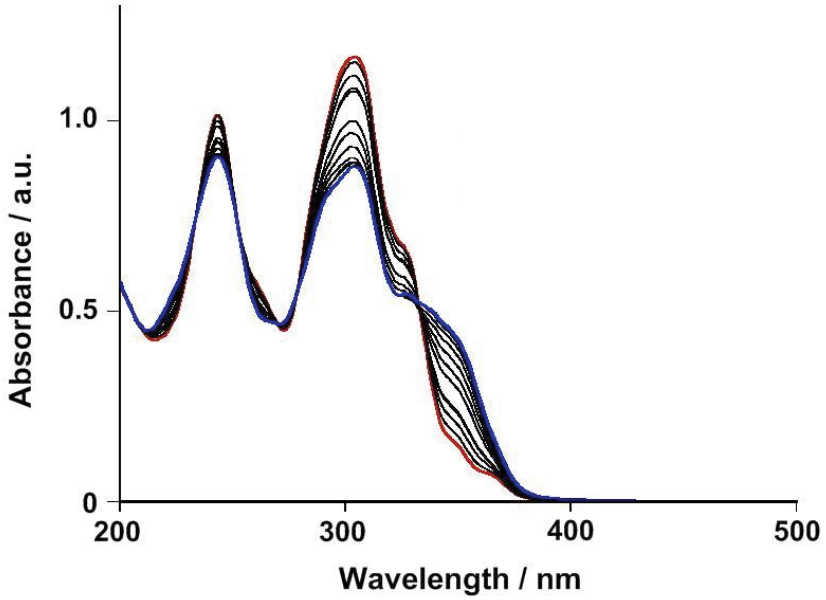

Fig. S7 Observed UV-vis absorption spectral changes upon addition of Zn^{2+} [0 mol dm^{-3} (red line) – 2.1 × 10^{-4} mol dm^{-3} (blue line)] to a MeCN solution of ImBrCz (3.1 × 10^{-4} mol dm^{-3}) at 298 K.

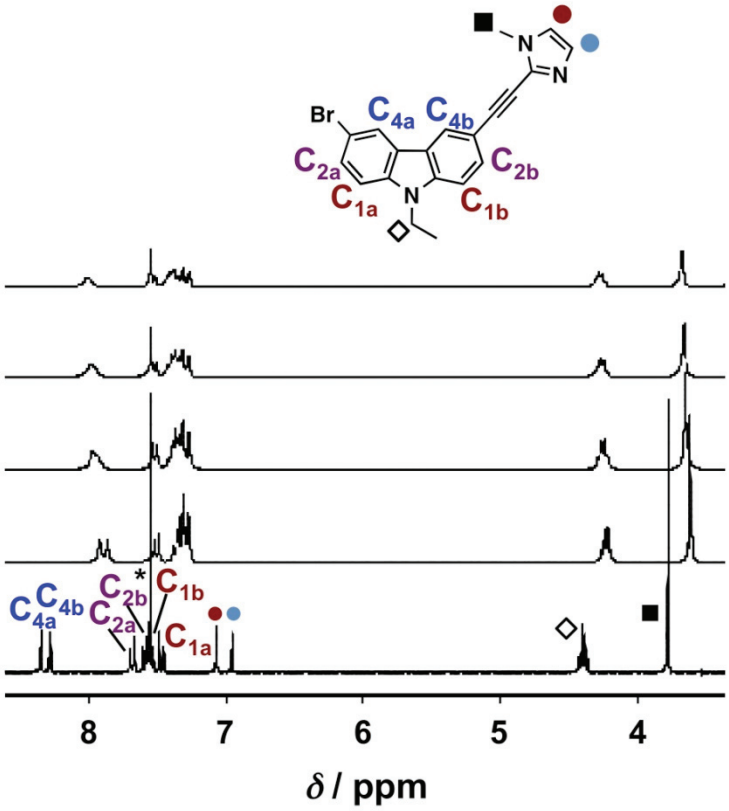

Fig. S8 Stacked plot of ^{1}H NMR spectra of ImBrCz (1.7×10^{-2} mol dm^{-3}) in the absence and presence of 0.05, 0.24, 0.31, and 0.50 equivalents of Zn^{2+} (from bottom to top) in CD_3CN at 298 K. Numbers and symbols correspond to those in the chemical structure of ImBrCz.

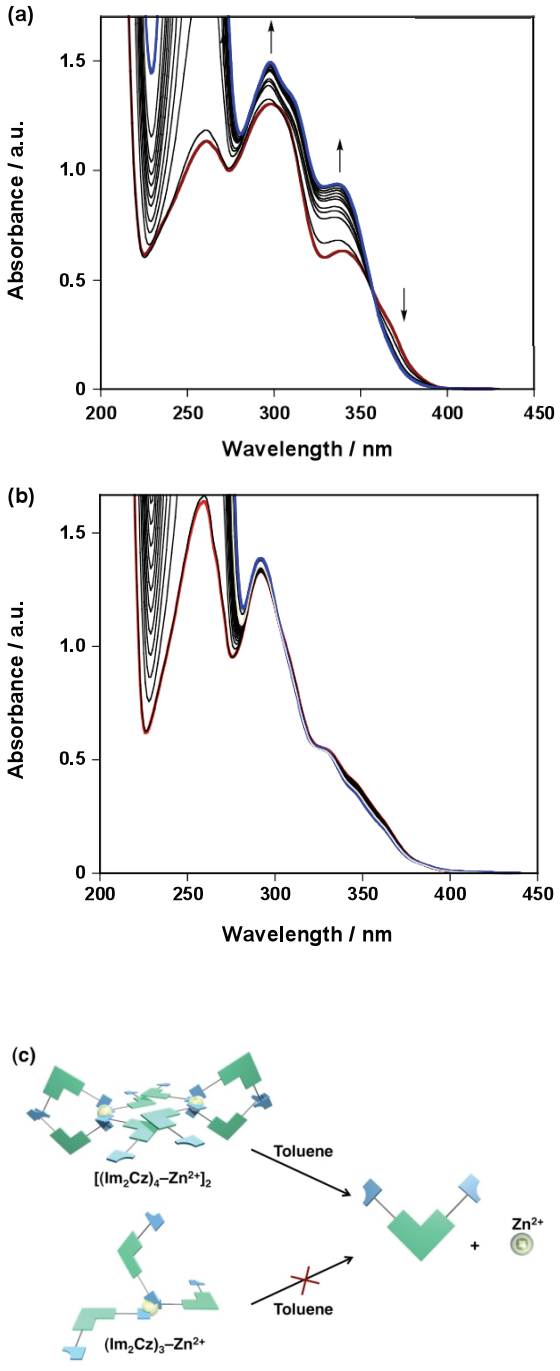

Fig. S9 Observed UV-vis absorption spectral changes of (a) Im_2Cz (3.4×10^{-4} mol dm^{-3}) in the presence of Zn^{2+} (1.0×10^{-4} mol dm^{-3}) upon addition of toluene (0 to 5.2×10^{-2} mol dm^{-3}) and (b) Im_2Cz (2.5×10^{-4} mol dm^{-3}) in the presence of Zn^{2+} (1.5×10^{-4} mol dm^{-3}) upon addition of toluene (0 to 9.6×10^{-2} mol dm^{-3}) in MeCN containing H_2O (0.22 mol dm^{-3}) at 298 K. (c) Schematic representation of dispersion of $[(Im_2Cz)_4–Zn^{2+}]_2$ (top) and $(Im_2Cz)_3–Zn^{2+}$ (bottom) into Im_2Cz and Zn^{2+} in the presence of toluene.

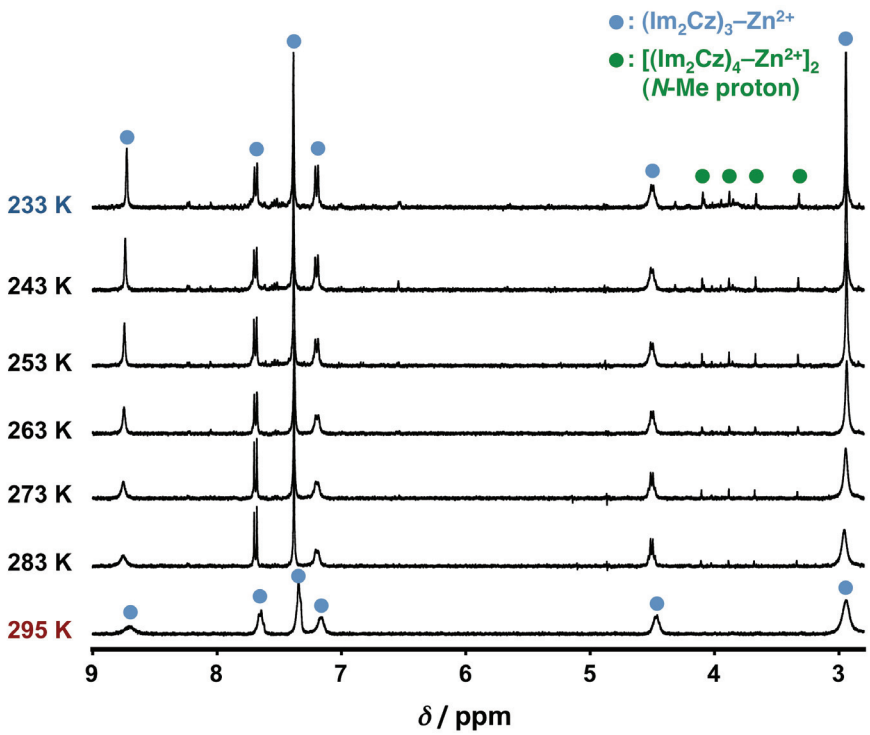

Fig. S10 ^{1}H NMR spectra of Im_2Cz (3.1×10^{-3} mol dm^{-3}) in the presence of Zn^{2+} (1.8×10^{-3} mol dm^{-3} in total) in CD_3CN at 233-295 K.

Table S11 Concentrations of $[(Im_2Cz)_4–Zn^{2+}]_2$, $(Im_2Cz)_3–Zn^2$, and free Zn^{2+}, equilibrium constant (K) of conversion of $[(Im_2Cz)_4–Zn^{2+}]_2$ into $(Im_2Cz)_3–Zn^2$ in CD_3CN solution of Im_2Cz (3.1×10^{-3} mol dm^{-3}) in the presence of Zn^{2+} (1.8×10^{-3} mol dm^{-3} in total) at 233-295 K.

T / K	$[[(Im_2Cz)_4–Zn^{2+}]_2]$ / mol dm^{-3} [a]	$[(Im_2Cz)_3–Zn^{2+}]$ / mol dm^{-3} [b]	Concentration of free Zn^{2+} / mol dm^{-3} [c]	K / mol^3 dm^{-9} [d]
233	5.4×10^{-5}	8.9×10^{-4}	8.0×10^{-4}	3.7×10^{-6}
243	3.9×10^{-5}	9.3×10^{-4}	7.9×10^{-4}	1.5×10^{-5}
253	3.1×10^{-5}	9.5×10^{-4}	7.8×10^{-4}	3.8×10^{-5}
263	2.5×10^{-5}	9.7×10^{-4}	7.8×10^{-4}	8.1×10^{-5}
273	1.9×10^{-5}	9.8×10^{-4}	7.8×10^{-4}	2.1×10^{-4}
283	*e*	9.8×10^{-4}	———	———
298	*e*	1.0×10^{-3}	———	———

[a] Determined by integration of the ^{1}H NMR signal at 3.30 ppm due to the *N*-Me protons of $[(Im_2Cz)_4–Zn^{2+}]_2$. [b] Determined by integration of the ^{1}H NMR signal at 4.46 ppm due to the CH_2 proton of $(Im_2Cz)_3–Zn^{2+}$. [c] Determined from the concentrations of $[(Im_2Cz)_4–Zn^{2+}]_2$, $(Im_2Cz)_3–Zn^2$, and Zn^{2+} in total (1.8×10^{-3} mol dm^{-3}). [d] Determined from eq 1. [e] Too small to be determined accurately.

$$K = \frac{[(Im_2Cz)_3–Zn^{2+}]^8}{[[(Im_2Cz)_4–Zn^{2+}]_2]^3[Zn^{2+}]^2} \quad (1)$$

$$3[(Im_2Cz)_4–Zn^{2+}]_2 \underset{}{\overset{Zn^{2+}}{\rightleftharpoons}} 8(Im_2Cz)_3–Zn^{2+}$$

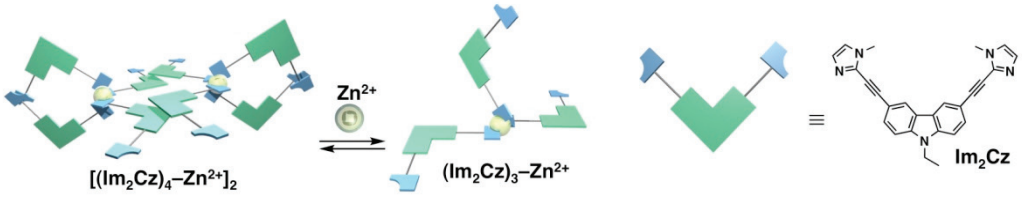

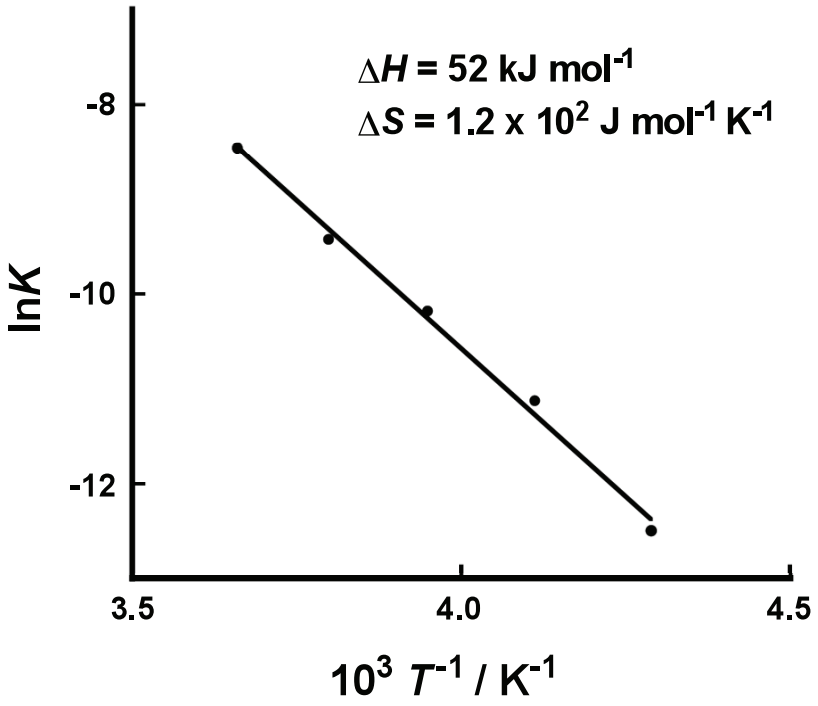

Fig. S12 Plot of ln *K* of the conversion of $[(Im_2Cz)_4–Zn^{2+}]_2$ into $(Im_2Cz)_3–Zn^{2+}$ *vs*. T^{-1}.